Rapid Dechlorination of Polychlorinated Dibenzo- p -dioxins by Bimetallic and Nanosized Zerovalent Iron

ARTICLE *in* ENVIRONMENTAL SCIENCE AND TECHNOLOGY · JULY 2008

Impact Factor: 5.33 · DOI: 10.1021/es702560k · Source: PubMed

Environ. Sci. Technol. **2008,** *42,* 4106–4112

Rapid Dechlorination of Polychlorinated Dibenzo-*p*-dioxins by Bimetallic and Nanosized Zerovalent Iron

JI-HUN KIM,[†] PAUL G. TRATNYEK,[‡] AND YOON-SEOK CHANG*,[†]

School of Environmental Science and Engineering, Pohang University of Science and Technology (POSTECH), Pohang, 790-784, South Korea and Department of Environmental and Biomolecular Systems, Oregon Health and Science University, Beaverton, Oregon 97006, USA

Received October 10, 2007. Revised manuscript received February 24, 2008. Accepted March 18, 2008.

Polychlorinated dibenzo-*p*-dioxins and furans (PCDD/Fs), especially the 2,3,7,8-substituted congeners, are extremely toxic, persistent, and recalcitrant to remediation. Dechlorination of PCDD/Fs by zerovalent iron (ZVI) is thermodynamically feasible, but useful rates of reaction have not been previously reported. Here we show that ZVI (both micro- and nanosized ZVI, without palladization) dechlorinates PCDD congeners with four or more chlorines in aqueous systems, but the reaction is too slow to achieve complete dechlorination within a practical period of time. In contrast, palladized nanosized ZVI (Pd/nFe) rapidly dechlorinates PCDDs, including the mono- to tetra-chlorinated congeners. The rate of 1,2,3,4-tetrachloro dibenzo-*p*-dioxin (1,2,3,4-TeCDD) degradation using Pd/nFe was about 3 orders of magnitude faster than 1,2,3,4-TeCDD degradation using unpalladized ZVI. The distribution of products obtained from dechlorination of 1,2,3,4-TeCDD suggests that palladization shifts the pathways of contaminant degradation toward a greater role of H atom transfer rather than electron transfer.

Introduction

Reductive dehalogenation using zerovalent iron (ZVI) has been extensively studied for the remediation of halogenated aliphatic contaminants, including carbon tetrachloride, 1,1,1-trichoroethane, and trichloroethylene (*1–3*). In contrast, few studies have examined the dehalogenation of halogenated aromatics by ZVI, and they involved only a limited range of chlorinated phenols (*4–6*), polybrominated diphenylethers (*7*), and polychlorinated biphenyls (*8*). The only published report on the dechlorination of polychlorinated dibenzo-*p*-dioxins (PCDDs) using ZVI is a preliminary study that we performed with PCDD/Fs-contaminated fly ash (*9*).

The toxicity of PCDD/F congeners varies greatly, with 2,3,7,8-TeCDD being the most toxic, so incomplete dechlorination starting with the more highly chlorinated PCDD/Fs can increase the net toxicity of mixtures. To avoid this, effective remediation of PCDD/Fs requires not only fast dechlorination of the parent compounds but also rapid conversion of the parent compounds to nontoxic products. With a variety of environmentally relevant reductants, dechlorination by dissociative electron transfer is thermodynamically favorable for all chlorines on all PCDD/Fs congeners (*10, 11*). However, the kinetics of PCDD dechlorination are expected to be slow, based on analogy to other chlorinated aromatics (*12, 13*) and on the available data for reductive dechlorination of PCDDs. The dechlorination of PCDD/Fs has been reported for pure (*14*) and mixed (*15*) cultures of anaerobic bacteria, anaerobic cultures with added electron transfer mediators (*16, 17*), and abiotic systems like ZVI in subcritical water (*18*). Recently, we reported that only 2% of 1,2,3,4-TeCDD was dechlorinated after 50 days, using microscale ZVI (*9*). None of these studies showed fast dechlorination or deep dechlorination (e.g., to the fully dechlorinated product, dibenzo-p-dioxin, DD). Thus, there is a continuing need for better ways to remediate PCDD/Fs under reducing conditions.

Two of the most successful strategies for enhancing the reactivity of dechlorination by ZVI involve nanosize particles of ZVI (nZVI) and bimetallic combinations of ZVI combined with catalytic, noble metals, such as Pd and Ni (*19, 20*). nZVI has been shown to reduce several chlorinated aromatics, including chlorinated phenols (*21*) and PCBs (*8, 22*). Bimetallic ZVI generally improves the degradation rates of polychlorinated biphenyls (*8, 23, 24*) and benzenes (*25, 26*), although an early study found that Pd/Fe lowered the rate of pentachlorophenol reduction (*6*).

In the study reported here, we sought to determine the kinetics and pathways of PCDD degradation using ZVI and nZVI, with and without palladization. We evaluated the types of iron in terms of dechlorination kinetics and the environmental acceptability of the dechlorinated products. Also, the kinetics and pathways obtained using the various iron types are compared, and mechanisms for PCDD dechlorination by ZVI and palladized ZVI are proposed.

Experimental Methods

Chemicals. All PCDDs congeners used in our dechlorination experiments and as standards for our analysis of the dechlorinated products were obtained from Accustandard (New Haven, CT; 99%+ pure). Acetone, toluene, isooctane, and methanol (Merck, Whitehouse Station, NJ; 99.9% pure, HPLC grade) were used to extract and analyze PCDDs. Hexachlorobenzene (HCB) and 1,2,3,4-tetrachloronaphthalene (1,2,3,4-TeCN) (Aldrich, Milwaukee, WI) were used for the internal standard and recovery standard. $FeCl_3 \cdot 6H_2O$ (Kanto, Japan), $NaBH_4$ (Aldrich), and Pd(II)-acetate (Aldrich) were used to synthesize palladized nZVI. All reaction vials in this research were silanized with 1,1,1,3,3,3-hexamethyldisilazane (HMDS) (Aldrich, 98% pure) before use. All chemicals were used as received. All solutions were prepared with water that was obtained from a Barnstead Nanopure system and then degassed by purging with argon for 2 h.

Preparation and Characterization of ZVI and Bimetallic ZVI. The microscale iron (mFe^{EL}) that we used for dechlorination was 100-mesh electrolytic Fe^0 powder (99% + purity; Fisher Scientific, Fair Lawn, NJ), and it was used as received. Nanoscale iron (nFe^{BH}) was synthesized from $FeCl_3 \cdot 6H_2O$ (0.15 M) by reduction with $NaBH_4$ (0.24 M), following established procedures (*22, 27*), except that we did not include drying and aging steps. Instead, we did each experiment by preparing and using the nFe^{BH} in one vial. The iron dosage was controlled by the amount of $FeCl_3 \cdot 6H_2O$ solution used (replicates showed that the variability in dry weight of nFe^{BH} resulting from this procedure was ± 1%). After the nFe^{BH} particles formed, the remaining $NaBH_4$ solution was decanted

* Corresponding author e-mail: yschang@postech.ac.kr; phone: +82-54-279-2281; fax: +82-54-279-8299.
[†] Pohang University of Science and Technology.
[‡] Oregon Health and Science University.

10.1021/es702560k CCC: $40.75
Published on Web 05/06/2008

TABLE 1. Physical and Chemical Properties of Irons

	type	N_2BET-surface area (m^2/g)[a]	elemental composition (wt %)[b]
mFe^{EL}	electrolytic Fisher iron	0.10 ± 0.01	Fe > 99[c]
Pd/mFe^{EL}	palladized mFe^{EL}	0.09 ± 0.01	Fe 87 O 12 Pd 0.6[d]
nFe^{BH}	reduction of $FeCl_3 \cdot 6H_2O$ by sodium borohydride	33.2 ± 1.2	Fe 44 O 50 B 6
Pd/nFe^{BH}	palladized nFe^{BH}	33.6 ± 1.3	Fe 39 O 55 B 5 Pd 0.5[d]

[a] From duplicate measurements. [b] Fe, O, B, and Pd were measured with XPS using the Scofield method. [c] From the Fisher product-information sheet. [d] The amount of Pd that was reanalyzed using ICP.

from the vial, and the nFe^{BH} was rinsed two times with degassed water while applying a strong magnet to retain the iron particles in the vial.

Palladization was performed electrochemically, following established procedures (*23, 28*). An aliquot (10−3000 μL) of deoxygenated, 5-mM Pd(II)-acetate solution was added to the bottles containing mFe^{EL} or nFe^{BH}, and the mixture was allowed to react for 30 min on an orbital mixer. The palladized iron was then rinsed 3 times to remove the remaining Pd(II)-acetate. To control the Pd concentration of the iron particles, a calibration was obtained by adding various amounts of Pd to the iron particles and determining the Pd/Fe ratio (w/w) with inductively coupled plasma emission spectroscopy (ICP). In most dechlorination experiments, 0.5% Pd/Fe (w/w) was used. The materials obtained by the palladization procedure described above are represented by Pd/mFe^{EL} and Pd/nFe^{BH} in this paper.

The composition and structure of the nFe^{BH} and Pd/nFe^{BH} were characterized by transmission electron microscopy (TEM; JEOL, Ltd., 4000FX) and electron dispersive X-rays (EDX) operated at 400 kV. For TEM analysis, 300-mesh Cu TEM grids with a carbon film were dipped into acetone that contained the dispersed nFe^{BH} or Pd/nFe^{BH}. The specific surface areas of mFe^{EL}, nFe^{BH}, Pd/mFe^{EL}, and Pd/nFe^{BH} were determined by BET N_2 gas adsorption (BELSORP-max; Japan). The elemental compositions of the four types of iron were determined by X-ray photoelectron spectroscopy (XPS; ESCA Laboratory 220iXL) using a Mg Kα line (1253.6 eV) as an excitation source and using ICP-atomic emission spectrometry (ICP-AES; Varian).

Dechlorination Experiments and Analysis. To initiate dechlorination experiments, 30−200 nmol of PCDDs (1,2-DiCDD, 1,2,3-TriCDD, or 1,2,3,4-TeCDD) in acetone was injected into the reaction vials containing the iron, and the acetone was evaporated under a stream of argon. The vials were then filled with 20 mL of degassed deionized water, leaving ~1 mL of headspace unfilled to control pressure in the vials (due to H_2 produced during corrosion of the Fe^0). The vials were sealed with the Teflon-lined septa inserted screw-caps and placed on a rolling mixer (15 rpm) in a dark room at room temperature until they were extracted for analysis. All samples with iron were prepared in triplicates; control samples without iron were prepared in duplicate.

After the desired reaction time (0−2 years for mFe^{EL} and nFe^{BH}, 0−2 days for Pd/mFe^{EL} and Pd/nFe^{BH}), the reaction vials were sacrificed for analysis. The aqueous phase in each reaction vial was decanted into 30 mL glass tubes with the iron particles held back via a strong magnet, and both phases (aqueous and particle) were spiked with HCB to serve as an internal standard. The aqueous phase was extracted with toluene, and the extracts were transferred to autosampler vials. The particle phase was dried by sonicating for 5 min in acetone twice, then once in a mixture of toluene/acetone (1:2 v/v), and then extracted as described above. Before analysis, 1,2,3,4-TeCN was added to the autosampler vials containing the extracts to serve as the recovery standard. In separate control experiments, the extraction recoveries were found to be more than 85%.

The identification and the quantification of the initial congeners and their dechlorinated products were performed by gas chromatography (column: DB5-MS, 30 m × 0.25 mm, 0.25 μm) with ion-trap mass spectrometry (IT-MS; Finnigan, Model: Polaris Q). However, the concentrations of the congeners formed by dechlorination of PCDDs with unpalladized iron (mFe^{EL} and nFe^{BH}) were too low to be detected using IT-MS, so these samples were analyzed by high-resolution GC with high-resolution MS (HRGC-HRMS, GC: HP6890, MS: 700T, JEOL) using a DB-5MS column (60 m × 0.25 mm, 0.25 μm).

Three-point calibrations were used to obtain the response factors for all PCDD congeners included in this study (1,2,3,4-TeCDD; 1,2,3- and 1,2,4-TriCDD; 1,2-, 1,3-, 1,4-, and 2,3-DiCDD; 1- and 2-MCDD; and DD). The approximate detection limits were 10 picomoles (pmol) with IT-MS and 10 attomoles (amol) with HR-MS.

Results and Discussion

Iron Characterization and the Effects of Pd on Iron Properties. The specific surface area and the chemical compositions of mFe^{EL}, nFe^{BH}, Pd/mFe^{EL}, and Pd/nFe^{BH} obtained with XPS and ICP analysis are given in Table 1. The results are generally in agreement with previous reports on comparable materials (e.g., refs *8, 22, 26−27*). Palladization did not change the specific surface areas of the materials. The Pd 3d region of the XPS spectra (data not shown) includes only peaks at Pd $3d_{3/2}$ (340.3 eV) and Pd $3d_{5/2}$ (335.0 eV), confirming, as found by others (*28*), that Pd^{2+} is reduced to Pd^0 on the iron surface. The TEM images of nFe^{BH} (Figure 1A) show that the fresh, unpalladized particles consist of roughly spherical cores covered with a shell that is uniformly 2−3 nm thick. The core/shell structure resulting from borohydride reduction has been shown (for similar materials) to consist predominantly of α-Fe^0 and a mixture of iron oxides and borates (*29*). In contrast, the shell of the palladized nFe^{BH} (Figure 1B) had a very different morphology; its oxide shell was thicker (10−30 nm) and less uniform, which is consistent with the effect of bimetal plating on other types of nZVI (*30*). Figure 1B includes EDX obtained at two places in the image domain, and these show that the Pd is localized in a rough, outer layer, which is similar to morphologies that have been reported previously (*26, 31*).

Kinetics of PCDD Dechlorination. Over 2 months of reaction, nFe^{BH} and mFe^{EL} did not produce any dechlorinated products from 1,2-DiCDD and 1,2,3-TriCDD, whereas the same treatments using 1,2,3,4-TeCDD gave quantifiable amounts of dechlorinated intermediates (MCDD to TriCDD)

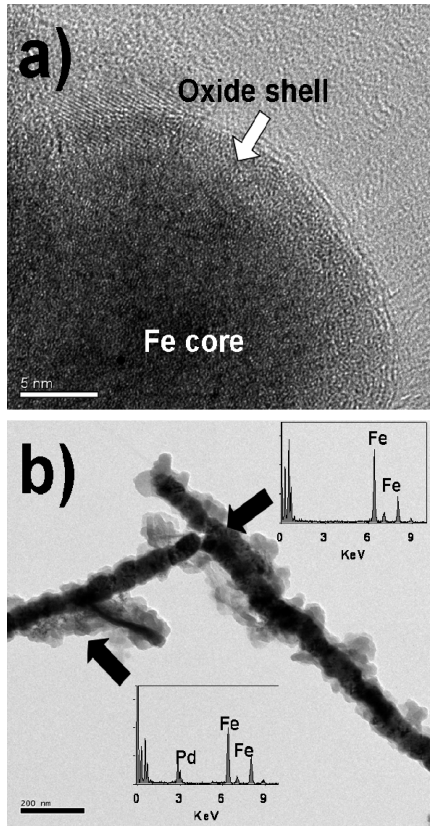

FIGURE 1. (A) Core−shell morphology and formation of nFe^{BH} oxide film (1 000 000×); (B) aggregates of Pd/nFe^{BH} and EDX spectra of the pointed spots (25 000×).

and of the fully dechlorinated product, DD (Figure 2A). The sum of dechlorinated products from 1,2,3,4-TeCDD, however, was only ~2 mol% of the initial 1,2,3,4-TeCDD (after 50 days of reaction time). Further analysis of PCDD dechlorination using mFe^{EL} over 2 years showed no further change in the distribution of the dechlorinated products, but the recoverable quantity of 1,2,3,4-TeCDD continued to decline, eventually resulting in a total mass balance of all PCDDs congeners that was ~40% (after 2 years). This decline in mass balance has also been observed in experiments with nZVI and PCBs (*8*), where it was attributed to the irreversible adsorption of the initial congener to the walls of glass vials and the Teflon-lined septa. In this case, we conclude that most of the unrecoverable TeCDD was irreversibly adsorbed onto unreactive areas of the ZVI, because control experiments done without iron produced only a 20% decline in mass balance for TeCDD (over 60 days).

Our finding that tetra- (or higher) chlorinated congeners reduce more rapidly rather than tri- and dichlorinated congeners is consistent with structure−activity relationships showing that dechlorination rates generally correlate with the degree of chlorination of halogenated organics (*32*), and that the degree of chlorination generally correlates with the reduction potential of closely related halogenated organics (*33*). The redox potentials of all 288 theoretically possible dechlorination reactions for 80 chlorinated dioxin congeners were calculated by Huang et al. (*11*), and the highest redox potential among these is between 1,2,3,4-TeCDD and 1,2,4-TriCDD. This result suggests that rates of dechlorination by nanoiron may not be significantly faster for the more highly chlorinated dioxin congeners. To test this, we currently are investigating the reduction of dioxin congeners with more than four chlorine substituents using nFe^{BH}.

Palladization increased the rate of dechlorination for all PCDDs studied. Pd/mFe^{EL} and Pd/nFe^{BH} dechlorinated 90%

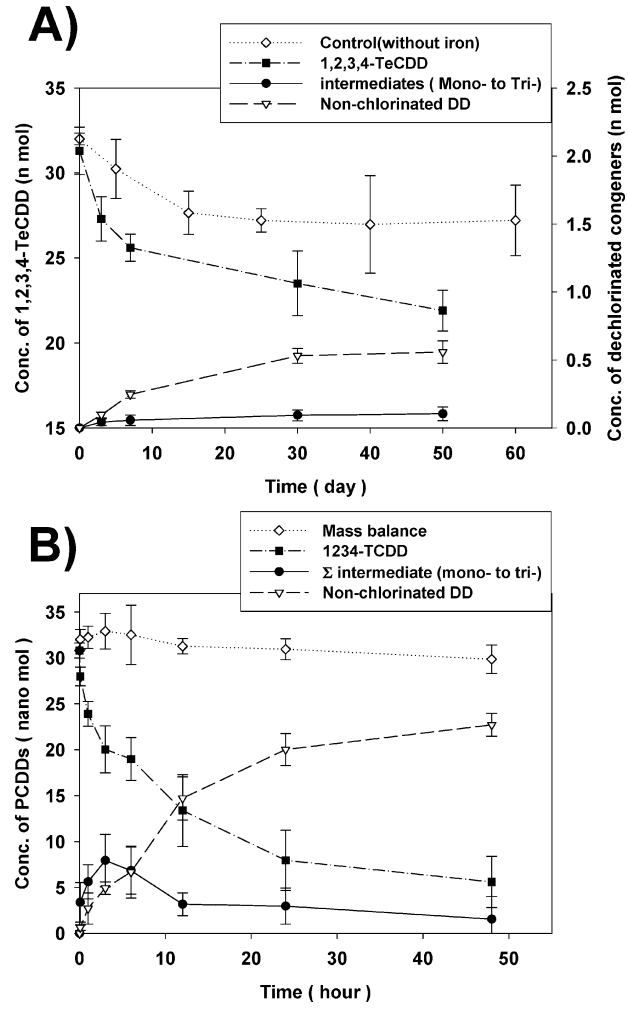

FIGURE 2. Degradation of 1,2,3,4-TeCDD (initial concentration = 31.1 nmol) by (A) mFe^{EL} (0.4 g of microsized iron), and (B) Pd/nFe^{BH} (0.1 g of nanosize iron, 0.5% Pd).

of 1,2,3,4-TeCDD to DD in 48 h, with pseudo first-order rate constants (k_{obs}) equal to $(3.3 \pm 0.8) \times 10^{-2}$ h^{-1} and $(5.1 \pm 1.3) \times 10^{-2}$ h^{-1}, respectively (Table 2). For 1,2,3,4-TeCDD, the dechlorination rate was almost 3 orders of magnitude greater than that for the unpalladized iron. Figure 2B shows the time profile for reaction of 1,2,3,4-TeCDD with Pd/nFe^{BH}. The yield of the intermediates (tri- to mono-) peaks became maximum at about 3 h and then gradually decreased. DD gradually accumulated and accounted for most of the products after two days of reaction. The overall mass balance for three sets of experiments was 103 ± 12%. The data (including data not shown for each intermediate congener, separately) implies stepwise dechlorination. Dechlorination rates were faster for the less-chlorinated congeners: 1.5−5 times faster for 1,2,3-TriCDD compared with 1,2,3,4-TeCDD (Figure 3), and 2−4 times faster for 1,2-DiCDD compared with 1,2,3-TriCDD (Table 2). Such differences in dechlorination rates, which are opposite from those described above for the structure−activity relationships in dechlorination of PCDDs by nFe^{BH} and mFe^{EL}, have also been observed for PCBs and palladized granular iron (*8*) and chlorinated ethenes reacting with nanoscale (*34*) and microscale iron (*35*).

It is difficult to quantitatively assess the benefits of palladization because some key factors that should be normalized are not generally known, such as the proportion of particle surface area that Pd occupies (*36*). Nevertheless, the large increases in dechlorination rates observed in our study seem to be larger than those that have been previously reported for comparable systems. For example, palladization

TABLE 2. The First-order PCDDs Dechlorination Rate Constants (k_{obs}) and Surface Area Normalized PCDDs Dechlorination Rate Constants (k_{sa}) of mFe^{EL}, nFe^{BH}, Pd/mFe^{EL}, and Pd/nFe^{BH}

	unpalladized iron				palladized iron			
	mFe^{EL}		nFe^{BH}		Pd/mFe^{EL}		Pd/nFe^{BH}	
	k_{obs} (h^{-1})[a]	k_{sa} ($Lh^{-1}m^{-2}$)[b]	k_{obs} (h^{-1})[a]	k_{sa} ($Lh^{-1}m^{-2}$)[b]	k_{obs} (h^{-1})[a]	k_{sa} ($Lh^{-1}m^{-2}$)[b]	k_{obs} (h^{-1})[a]	k_{sa} ($Lh^{-1}m^{-2}$)[b]
1,2,3,4-TeCDD	$1.7 \pm 0.4 \times 10^{-5}$	$8.7 \pm 2.0 \times 10^{-6}$	$3.7 \pm 1.3 \times 10^{-5}$	$2.2 \pm 0.8 \times 10^{-7}$	$3.3 \pm 0.8 \times 10^{-2}$	$1.9 \pm 0.4 \times 10^{-2}$	$5.1 \pm 1.3 \times 10^{-2}$	$3.0 \pm 0.9 \times 10^{-4}$
1,2,3-TriCDD	ND[c]	ND	ND	ND	$5.2 \pm 1.5 \times 10^{-2}$	$2.9 \pm 0.9 \times 10^{-2}$	$2.6 \pm 0.4 \times 10^{-1}$	$1.5 \pm 0.3 \times 10^{-3}$
1,2-DiCDD	ND	ND	ND	ND	$2.3 \pm 0.4 \times 10^{-1}$	$1.3 \pm 0.2 \times 10^{-1}$	$4.5 \pm 0.6 \times 10^{-1}$	$2.7 \pm 0.5 \times 10^{-3}$

[a] Reported uncertainties are 95% confidence intervals for pseudo first-order fit of product data. [b] Reported uncertainties are calculated from 95% confidence limits using errorpropagation methods. [c] Not determined.

FIGURE 3. Degradation of 1,2,3-TriCDD (initial concentration = 34.78 nmol) by mFe^{EL} (0.4 g), nFe^{BH} (0.1 g), Pd/mFe^{EL} (0.4 g, 0.5% Pd), and Pd/nFe^{BH} (0.1 g, 0.5% Pd).

of nZVI has been reported to increase dechlorination rates by 1.5−2 orders of magnitude for PCBs and chlorinated benzenes (*8, 25*) and to decrease dechlorination rates by 1 order of magnitude for pentachlorophenol (*6*). For halogenated aliphatics, it has been shown that the increase in reduction rates due to palladization is significantly affected by the pattern of chlorination even within a set of congeners (*37*). Our data are consistent with these observations, showing that palladization increased rates of PCDD dechlorination in all cases.

Another example of the difficulty comparing quantitatively the PCDD declorination rates for the different types of reductants studied here involves determining if there is a benefit to using nanosized iron instead of the microsized iron. On the basis of k_{obs}, Pd/nFe^{BH} yielded degradation rates for PCDDs congeners that were 2−5 times greater than for Pd/mFe^{EL}. However, the surface area normalized rate constants (k_{sa}, calculated using the BET-specific surface areas) given in Table 1 suggest that $Pd\text{-}mFe^{EL}$ is about 20−60 times more reactive than Pd/nFe^{BH}. We have recently shown that nanosize does not necessarily impart higher reactivity when comparisons are made on a (total) surface area basis (*38*). However, in this case, the lower k_{sa} obtained with Pd/nFe^{BH} compared to Pd/mFe^{EL} are likely due to differences in how the Pd is distributed on the surface of the iron particles, which is not a factor that is readily quantified.

Despite the relatively high rates of PCDDs dechlorination by Pd/nFe^{BH}, our data suggest that a small fraction of the PCDD is recalcitrant to degradation over considerable exposure times. After 2 days, we could not account for 10% of initial 1,2,3,4-TeCDD, 5% of 1,2,3-TriCDD, and 2% of 1,2-DiCDD (Figures 2B and 3). These residues may have been adsorbed to the vial walls, to the septa liner, or to unreactive sites on the iron surface caused by heterogeneous plating of Pd (Figure 1B). However, losses to the silanized glass vials should have been negligible over 2 days, so we favor the hypothesis that PCDD residues were sequestered onto nonreactive surface areas of Pd/nFe^{BH}. This hypothesis is consistent with the observation that the amount of sequestered PCDD increases with the degree of chlorination (which is accompanied by decreased solubility (*39*)).

Dechlorination Pathways of PCDDs. The main dechlorination pathway of 1,2,3,4-TeCDD by unpalladized iron (mFe^{EL} and nFe^{BH}) was 1,2,3,4-TeCDD → 1,2,4-TriCDD → 1,3-DCDD → 2-MCDD (Figure 4A and Table 3). This pathway is consistent with that proposed by Huang et al. (*11*), based on calculated difference between the free energies for each

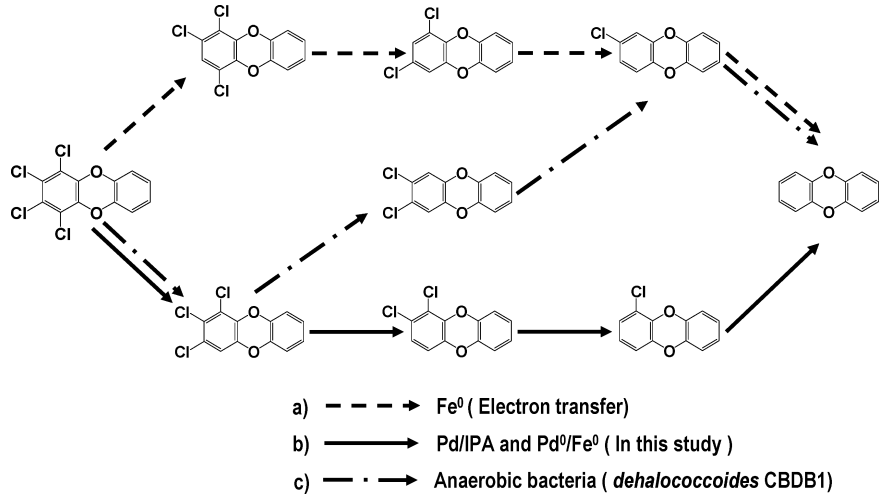

FIGURE 4. Comparison of dechlorination pathways for 1,2,3,4-TeCDD.

TABLE 3. Distribution of Dechlorinated Products[a]

		1,2,3,4-TeCDD		1,2,3-TriCDD	1,2-DiCDD
products		unpalladized	palladized	palladized	palladized
Tri-	123	37 ± 4	**77 ± 8**		
	124	**63 ± 4**	23 ± 8		
Di-	12	14 ± 2	**75 ± 7**	**51 ± 9**	
	13	**44 ± 3**	4 ± 2	6 ± 3	
	14	28 ± 3	5 ± 2		
	23	14 ± 2	16 ± 4	43 ± 10	
Mono-	1	38 ± 4	**69 ± 11**	**61 ± 12**	**54 ± 15**
	2	**62 ± 5**	31 ± 11	39 ± 12	46 ± 15

[a] Each number is the percentage of the dechlorinated products for each homologue; standard deviation was estimated from triplicates. Bold indicates the major congener for each homologue.

possible reductive dechlorination step. This agreement suggests that dissociative electron transfer probably is the dominant pathway for dechlorination of 1,2,3,4-TeCDD by unpalladized iron. Another rationale for the observed pattern of dechlorination comes from calculated properties of each C−Cl bond. Calculations done with density functional theory show that the lateral chlorines (2-, 3- positions) on PCDDs have greater intramolecular Cl−Cl repulsion energies than the peri-chlorines (1-, 4- positions) (*40*). Therefore, steric repulsion favors dissociation of the C−Cl bonds in the lateral positions, which is consistent with the pattern of sequential dechlorination steps that we observed with unpalladized iron.

This pattern of reactivity has implications for remediation. Dechlorination of PCDDs by unpalladized iron apparently favors less toxic products because the initial step removes lateral-chlorines preferentially, as expected for reduction by dissociative electron transfer. In contrast, dissociative electron transfer is usually presumed to be responsible for dechlorination when it results from the metabolism of anaerobic bacteria, but *dehalococcoides* sp. strain CBDB1, one species that can perform dehalorespiration of PCDDs, initially removes peri- rather than lateral-chlorines (Figure 4C) (*14*). The removal of peri-chlorines from higher chlorinated dioxins causes the formation of 2,3,7,8-substituted congeners, which increases the toxicity of the mixture.

The main dechlorination pathway of 1,2,3,4-TeCDD by palladized iron (Pd/mFe^{EL} and Pd/nFe^{BH}) was 1,2,3,4-TeCDD → 1,2,3-TriCDD → 1,2-DiCDD → 1-MCDD (Figure 4B). The difference between this pathway and the one observed for unpalladized iron is a more notable effect of palladization on the pathway of dechlorination than has been previously reported. The pathway of dechlorination that we observed with palladized iron and 1,2,3,4-TeCDD is not the thermodynamically favored route for dissociative electron transfer, but it is consistent with the pathway reported for PCDD dechlorination in alkaline isopropyl alcohol (IPA) with Pd catalysts (*39*). Dechlorination by the Pd/IPA system is believed to involve the transfer of hydrogen—donated by the α-hydrogen in IPA, catalyzed on the Pd surface, and involving H (atomic or "nascent" hydrogen) or possibly H^- (hydride) and not electron transfer (*41*). Therefore, a similar mechanism might be involved in the reduction of 1,2,3,4-TeCDD by palladized iron, as reported here.

The relative significance of electron transfer versus hydrogen atom transfer has long been part of the debate over why palladized iron (and other bimetallic combinations of ZVI with noble, catalytic metals) often reduces contaminants more rapidly and to more desirable products than unpalladized ZVI. It has been implied that contaminant reduction by electron transfer is accelerated by Galvanic coupling between the iron and noble metal (*25*), but Galvanic coupling also increases the rate at which H_2O/H^+ is reduced to H_2 (the anoxic/aqueous corrosion reaction), which occurs via absorbed atomic hydrogen (H_{ads}), which, in turn, can contribute to increased rates of contaminant reduction (*37, 42*). Our data on the pathways of PCDD reduction support the latter interpretation of the bimetallic effect: that Galvanic coupling favors formation of activated H-species, and reduction by these species is responsible for accelerated rates of contaminant reduction.

Another argument in favor of H-atom transfer as the dominant pathway in PCDD dechlorination by palladized iron can be made on steric considerations. The distance between the atomic nuclei of neighboring chlorines in a dioxin molecule is about 3−4 Å (*43*) and the size of an H atom is about 1 Å, so steric hindrance could inhibit the formation of any precursor complex between H atom and PCDDs. Steric effects are not, however, expected to have as much effect on dechlorination by electron transfer, because the rate limiting step (electron attachment) precedes any atom transfer steps. Once again, the observed pattern of PCDD dechlorination by Pd/Fe favors the H atom transfer mechanism, because the chlorines that are least hindered by neighboring chlorines (the 1,4-positions of 1,2,3,4-TeCDD, and 1,3-positions of 1,2,3-TriCDD) are the positions that are dechlorinated most rapidly.

These mechanistic considerations are advantageous for PCDD degradation by unpalladized iron, because preferential removal of the lateral chlorines lowers the overall toxicity of the PCDD mixtures. With palladized iron, however, PCDD

dechlorination is faster and proceeds farther, which also can reduce overall toxicity. Additional data are needed to verify these results with other PCDD congeners and with PCDFs. We are currently developing a dechlorination procedure using Pd/Fe for the disposal of fly ash and soils contaminated with PCDD/Fs.

Acknowledgments

This work was supported by POSCO, the Korea Ministry of Environment, as "The Eco-technopia 21 project" (020-051-010) and a Korea Research Foundation grant funded by the Korean Government (MOEHRD) (KRF-2006-612- D00052). We thank J. Nurmi for his suggestions throughout this work.

Literature Cited

(1) Gillham, R. W.; O'Hannesin, S. F. Enhanced degradation of halogenated aliphatics by zero-valent iron. *Ground Water* **1994**, *32*, 958–967.

(2) Johnson, T. L.; Scherer, M. M.; Tratnyek, P. G. Kinetics of halogenated organic compound degradation by iron metal. *Environ. Sci. Technol.* **1996**, *30*, 2634–2640.

(3) Miehr, R.; Tratnyek, P. G.; Bandstra, J. Z.; Scherer, M. M.; Alowitz, M. J.; Bylaska, E. J. Diversity of contaminant reduction reactions by zerovalent iron: Role of the reductate. *Environ. Sci. Technol.* **2004**, *38*, 139–147.

(4) Morales, J.; Hutcheson, R.; Cheng, I. F. Dechlorination of chlorinated phenols by catalyzed and uncatalyzed Fe(0) and Mg(0) particles. *J. Hazard. Mater.* **2002**, *90*, 97–108.

(5) Ravary, C.;. Lipczynska-Kochany, E. Abiotic aspects of zero-valent iron induced degradation of aqueous pentachlorophenol In *Preprint Extended Abstracts, Division of Environmental Chemistry, 209th National Meeting*; American Chemical Society: 1995; Vol *35*, pp738−740.

(6) Kim, Y. H.; Carraway, E. R. Dechlorination of pentachlorophenol by zero valent iron and modified zero valent irons. *Environ. Sci. Technol.* **2000**, *34*, 2014–2017.

(7) Keum, Y. S.; Li, Q. X. Reductive debromination of polybrominated diphenyl ethers by zerovalent iron. *Environ. Sci. Technol.* **2005**, *39*, 2280–2286.

(8) Lowry, G. V.; Johnson, K. M. Congener-specific dechlorination of dissolved PCBs by microscale and nanoscale zerovalent iron in a water/methanol solution. *Environ. Sci. Technol.* **2004**, *38*, 5208–5216.

(9) Kim, J. H.; Lim, Y. K.; Chang, Y. S. Reductive dechlorination of PCDD/Fs on fly ash in aqueous solution using zero-valent iron metal, In *Preprint Extended Abstracts, Division of Environmental Chemistry, 228th National Meeting*; American Chemical Society: Philadelphia, Pennsylvania, 2004; Vol *44*, pp 235−238.

(10) Lynam, M. M.; Kuty, M.; Damborsky, J.; Koca, J.; Adriaens, P. Molecular orbital calculations to describe microbial reductive dechlorination of polychlorinated dioxins. *Environ. Toxicol. Chem.* **1998**, *17*, 988–997.

(11) Huang, C. L. I.; Keith Harrison, B.; Madura, J.; Dolfing, J. Gibbs free energies of formation of PCDDs: Evaluation of estimation methods and application for predicting dehalogenation pathways. *Environ. Toxicol. Chem.* **1996**, *15*, 824–836.

(12) Dolfing, J.; Harrison, B. K. Gibbs free energy of formation of halogenated aromatic compounds and their potential role as electron acceptors in anaerobic environments. *Environ. Sci. Technol.* **1992**, *26*, 2213–2218.

(13) Peijnenburg, W. J. G. M.; T Hart, M. J.; Den Hollander, H. A.; Van De Meent, D.; Verboom, H. H.; Wolfe, N. L. QSARs for predicting reductive transformation rate constants of halogenated aromatic hydrocarbons in anoxic sediment systems. *Environ. Toxicol. Chem.* **1992**, *11*, 301–314.

(14) Bunge, M.; Adrian, L.; Kraus, A.; Opel, M.; Lorenz, W. G.; Andreesen, J. R.; Görisch, H.; Lechner, U. Reductive dehalogenation of chlorinated dioxins by an anaerobic bacterium. *Nature* **2003**, *421*, 357–360.

(15) Adriaens, P.; Fu, Q.; Grbic-Galic, D. Bioavailability and transformation of highly chlorinated dibenzo-*p*-dioxins and dibenzofurans in anaerobic soils and sediments. *Environ. Sci. Technol.* **1995**, *29*, 2252–2260.

(16) Shiang Fu, Q.; Barkovskii, A. L.; Adriaens, P. Reductive transformation of dioxins: An assessment of the contribution of dissolved organic matter to dechlorination reactions. *Environ. Sci. Technol.* **1999**, *33*, 3837–3842.

(17) Adriaens, P.; Chang, P. R.; Barkovskii, A. L. Dechlorination of PCDD/F by organic and inorganic electron transfer molecules in reduced environments. *Chemosphere* **1996**, *32*, 433–441.

(18) Kluyev, N.; Cheleptchikov, A.; Brodsky, E.; Soyfer, V.; Zhilnikov, V. Reductive dechlorination of polychlorinated dibenzo-*p*-dioxins by zerovalent iron in subcritical water. *Chemosphere* **2002**, *46*, 1293–1296.

(19) Obare, S. O.; Meyer, G. J. Nanostructured materials for environmental remediation of organic contaminants in water. *J. Environ. Sci. Health* **2004**, *A39*, 2549–2582.

(20) Li, L.; Fan, M.; Brown, R. C.; van Leeuwen, J.; Wang, J.; Wang, W.; Song, Y.; Zhang, P. Synthesis, properties, and environmental applications of nanoscale iron-based materials: A review. *Crit. Rev. Environ. Sci. Technol* **2006**, *36*, 405–431.

(21) Cheng, R.; Wang, J. l.; Zhang, W.-X. Comparison of reductive dechlorination of p-chlorophenol using Fe^0 and nanosized Fe^0. *J. Hazard. Mater.* **2007**, *144*, 334–339.

(22) Wang, C. B.; Zhang, W.-X. Synthesizing nanoscale iron particles for rapid and complete dechlorination of TCE and PCBs. *Environ. Sci. Technol.* **1997**, *31*, 2154–2156.

(23) Grittini, C.; Malcomson, M.; Fernando, Q.; Korte, N. Rapid dechlorination of polychlorinated biphenyls on the surface of a Pd/Fe bimetallic system. *Environ. Sci. Technol.* **1995**, *29*, 2898–2900.

(24) Xu, J.; Bhattacharyya, D. Fe/Pd nanoparticle immobilization in microfiltration membrane pores: Synthesis, characterization, and application in the dechlorination of polychlorinated biphenyls. *Ind. Eng. Chem. Res.* **2007**, *46*, 2348–2359.

(25) Xu, Y.; Zhang, W.-X. Subcolloidal Fe/Ag particles for reductive dehalogenation of chlorinated benzenes. *Ind. Eng. Chem. Res.* **2000**, *39*, 2238–2244.

(26) Zhou, H. Y.; Xu, X. H.; Wang, D. H. Catalytic dechlorination of chlorobenzene in water by Pd/Fe bimetallic system. *J. Environ. Sci.* **2003**, *15*, 647–651.

(27) Glavee, G. N.; Klabunde, K. J.; Sorensen, C. M.; Hadjipanayis, G. C. Chemistry of borohydride reduction of iron(II) and iron(III) ions in aqueous and nonaqueous media. Formation of nanoscale Fe, FeB, and Fe_2B powders. *Inorg. Chem.* **1995**, *34*, 28–35.

(28) Muftikian, R.; Nebesny, K.; Fernando, Q.; Korte, N. X-ray photoelectron spectra of the palladium−iron bimetallic surface used for the rapid dechlorination of chlorinated organic environmental contaminants. *Environ. Sci. Technol.* **1996**, *30*, 3593–3596.

(29) Nurmi, J. T.; Tratnyek, P. G.; Sarathy, V.; Baer, D. R.; Amonette, J. E.; Pecher, K.; Wang, C.; Linehan, J. C.; Matson, D. W.; Penn, R. L.; Driessen, M. D. Characterization and properties of metallic iron nanoparticles: Spectroscopy, electrochemistry, and kinetics. *Environ. Sci. Technol.* **2005**, *39*, 1221–1230.

(30) Chun, C. L.; Baer, D. R.; Matson, D. W.; Amonette, J. E.; Penn, R. L. Characterizations and reactivity of metal-doped iron and magnetite nanoparticles. In *Preprint Extended Abstracts, Division of Environmental Chemistry, 233rd National Meeting*; American Chemical Society: Chicago, Illinois, 2007, Vol *47*, pp 408−412.

(31) Kim, Y. H.; Carraway, E. R. Dechlorination of chlorinated ethenes and acetylenes by palladized iron. *Environ. Tech.* **2003**, *24*, 809–819.

(32) Scherer, M. M.; Balko, B. A.; Gallagher, D. A.; Tratnyek, P. G. Correlation analysis of rate constants for dechlorination by zero-valent iron. *Environ. Sci. Technol.* **1998**, *32*, 3026–3033.

(33) Tratnyek, P. G.; Weber, E. J.; Schwarzenbach, R. P. Quantitative structure-activity relationships for chemical reductions of organic contaminants. *Environ. Toxicol. Chem.* **2003**, *22*, 1733–1742.

(34) Song, H.; Carraway., E. R. Catalytic hydrodechlorination of chlorinated ethenes by nanoscale zero-valent iron. *App. Catal., B.* **2008**, *78*, 53–60.

(35) Arnold, W. A.; Roberts., A. L. Pathways and kinetics of chlorinated ethylene and chlorinated acetylene reaction with Fe(0) particles. *Environ. Sci. Technol.* **2000**, *34*, 1794–1805.

(36) Cwiertny, D. M.; Bransfield, S. J.; Livi, K. J. T.; Fairbrother, D. H.; Roberts, A. L. Exploring the influence of granular iron additives on 1,1,1-trichloroethane reduction. *Environ. Sci. Technol.* **2006**, *40*, 6837–6843.

(37) Cwiertny, D. M.; Bransfield, S. J.; Roberts, A. L. Influence of the oxidizing species on the reactivity of iron-based bimetallic reductants. *Environ. Sci. Technol.* **2007**, *41*, 3734–3740.

(38) Tratnyek, P. G.; Johnson, R. L. Nanotechnologies for environmental cleanup. *Nano Today* **2006**, *1*, 44–48.

(39) Shiu, W. Y.; Doucette, W.; Gobas, F. A. P. C.; Andren, A.; Mackay, D. Physical-chemical properties of chlorinated dibenzo-*p*-dioxins. *Environ. Sci. Technol.* **1988**, *22*, 651–658.

(40) Lee, J. E.; Choi, W.; Mhin, B. J. DFT calculation on the thermodynamic properties of polychlorinated dibenzo-*p*-dioxins: Intramolecular Cl-Cl repulsion effects and their thermochemical implications. *J. Phys. Chem. A* **2003**, *107*, 2693–2699.

(41) Ukisu, Y.; Miyadera, T. Hydrogen-transfer hydrodechlorination of polychlorinated dibenzo-*p*-dioxins and dibenzofurans catalyzed by supported palladium catalysts. *App. Catal., B.* **2003**, *40*, 141–149.

(42) Schrick, B.; Blough, J. L.; Jones, A. D.; Mallouk, T. E. Hydrodechlorination of trichloroethylene to hydrocarbons using bimetallic nickel-iron nanoparticles. *Chem. Mater.* **2002**, *14*, 5140–5147.

(43) Hirokawa, S.; Imasaka, T.; Urakami, Y. Ab initio MO study on the S1←S0 transitions of polychlorinated dibenzo-*p*-dioxins. *J. Mol. Struct.: Theochem* **2003**, *622*, 229–237.

ES702560K